

Journal Pre-proof

Species-specific regulatory pathways of small RNAs play sophisticated roles in flower development in *Dimocarpus longan* Lour.

Bo Liu, Guanliang Li, Chengjie Chen, Zaohai Zeng, Jing Xu, Jisen Zhang, Rui Xia, Yuanlong Liu



PII: S2468-0141(22)00142-X

DOI: <https://doi.org/10.1016/j.hpj.2022.12.004>

Reference: HPJ 411

To appear in: *Horticultural Plant Journal*

Please cite this article as: Liu B, Li G, Chen C, Zeng Z, Xu J, Zhang J, Xia R, Liu Y, Species-specific regulatory pathways of small RNAs play sophisticated roles in flower development in *Dimocarpus longan* Lour., *Horticultural Plant Journal*, <https://doi.org/10.1016/j.hpj.2022.12.004>.

This is a PDF file of an article that has undergone enhancements after acceptance, such as the addition of a cover page and metadata, and formatting for readability, but it is not yet the definitive version of record. This version will undergo additional copyediting, typesetting and review before it is published in its final form, but we are providing this version to give early visibility of the article. Please note that, during the production process, errors may be discovered which could affect the content, and all legal disclaimers that apply to the journal pertain.

Copyright © 2022 Chinese Society for Horticultural Science (CSHS) and Institute of Vegetables and Flowers (IVF), Chinese Academy of Agricultural Sciences (CAAS). Publishing services by Elsevier B.V. on behalf of KeAi Communications Co. Ltd.

Species-specific regulatory pathways of small RNAs play sophisticated roles in flower development in *Dimocarpus longan* Lour.

Bo Liu^{a,b,c}, Guanliang Li^{a,b,c}, Chengjie Chen^{a,b,c}, Zaohai Zeng^{a,b,c}, Jing Xu^{a,b,c}, Jisen Zhang^d, Rui Xia^{a,b,c,*}, and Yuanlong Liu^{a,b,c,*}

^aState Key Laboratory for Conservation and Utilization of Subtropical Agro-Bioresources, South China Agricultural University, Guangzhou 510640, China

^bGuangdong Laboratory for Lingnan Modern Agriculture, South China Agricultural University, Guangzhou 510640, China

^cKey Laboratory of Biology and Germplasm Enhancement of Horticultural Crops in South China, Ministry of Agriculture and Rural Affairs, South China Agricultural University, Guangzhou 510640, China

^dCenter for Genomics and Biotechnology, Haixia Institute of Science and Technology, College of Life Sciences, Fujian Agriculture and Forestry University, Fuzhou 350002, China

Abstract

Flower development plays vital role in horticultural plants. Post-transcriptional regulation via small RNAs is important for plant flower development. To uncover post-transcriptional regulatory networks during the flower development in *Dimocarpus longan* Lour. 'Shixia', an economically important fruit crop in subtropical regions, we collected and analyzed sRNA deep-sequencing datasets and degradome libraries. Apart from identifying miRNAs and phased siRNA generating loci (*PHAS* loci), 120 hairpin loci, producing abundant sRNAs, were identified by in-house protocols. Our results suggested that 56 miRNA-target pairs, 22 21-nt-*PHAS* loci, and 111 hairpin loci are involved in post-transcriptional gene silencing during longan reproductive development. Lineage-specific or species-specific post-transcriptional regulatory modules have been unveiled, including miR482-*PHAS* and miRN15. miR482-*PHAS* might be involved in longan flower development beyond their conserved roles in plant defense, and miRN15 is a novel miRNA likely associated with a hairpin locus (*HPL-056*) to regulate strigolactone receptor gene *DWARF14* (*D14*) and the biogenesis of phasiRNAs from *D14*. These small RNAs are enriched in flower buds, suggesting they are likely involved in post-transcriptional regulatory networks essential for longan flower development via the strigolactone signaling pathway.

Keywords: *Dimocarpus longan* Lour.; Small RNAs; Flower development; Post-transcriptional regulation

* Corresponding authors.

E-mail addresses: rxia@scau.edu.cn; liuyuanlong@scau.edu.cn

Peer review under responsibility of Chinese Society of Horticultural Science (CSHS) and Institute of Vegetables and Flowers (IVF), Chinese Academy of Agricultural Sciences (CAAS)

<https://doi.org/10.1016/j.hpj>.

2468-0141/2022 Chinese Society for Horticultural Science (CSHS) and Institute of Vegetables and Flowers (IVF), Chinese Academy of Agricultural Sciences (CAAS). Production and hosting by Elsevier B.V. on behalf of KeAi Communications Co., Ltd. This is an open access article under the CC BY-NC-ND license. (<http://creativecommons.org/licenses/by-nc-nd/4.0/>)

1. Introduction

Longan (*Dimocarpus longan* Lour.) is an important economic fruit tree of the Sapindaceae family. Although it is native to southeast Asia, it is grown in many subtropical and tropical countries (Wang et al., 2015; Huang et al., 2021). As a fruit crop, floral formation and development greatly affect its yield; for instance, inflorescence architecture formation is closely related to fruit set (Lee and Chang, 2019) and flower sex differentiation. Moreover, longan ultimate female flowering rates are crucial for pollination success and stable yield (Huang et al., 2021). To date, comprehensive transcriptome analyses have been performed to investigate the underlying transcriptional regulatory mechanisms of longan flower development (Jia et al., 2014; Jue et al., 2019). However, studies aiming to uncover post-transcriptional regulations of longan flower development are scarce.

Small RNAs (sRNAs), one of the most important regulators at the post-transcriptional level, are predominantly 20–24 nucleotides (nt) in length in plants, and have been classified based on their distinct biogenesis, which include almost all aspects of plant development and defense (Borges and Martienssen, 2015). Among them, microRNAs (miRNAs) and phased small interfering RNAs (phasiRNA) are the most studied classes, for their essential roles in plant growth and development (Jiang et al., 2020; Sharma et al., 2020; Li et al., 2021, 2022; Zhang et al., 2022a, 2022b). In general, highly conserved miRNAs direct conserved regulatory modules and have similar functions across flowering plants. For example, miR156-*SQUAMOSA PROMOTER BINDING PROTEIN-LIKE (SPLs)*, miR172-*APETALA2 (AP2)*, and miR390-*TAS3-AUXIN RESPONSE FACTORS (ARFs)* are involved in floral transition or floral organ formation (Wang et al., 2009; Wu et al., 2009; Cho et al., 2013). miR2275, triggering the biogenesis of 24-nt reproductive phasiRNAs, is involved in anther and pollen development in many angiosperms (Xia et al., 2019). Some less conserved or lineage-specific miRNA might have unique functions in different species, such as miR528, which modulates flowering time and anti-virus response in rice (Yang et al., 2019; Yao et al., 2019), affects lodging resistance in maize (Sun et al., 2018), but responds to cold stress in banana fruits (Zhu et al., 2020). On the other hand, different miRNA from different species may be involved in similar or relevant biological processes, such as miR2118 in grass and miR11308 in Rosaceae species, which trigger the biogenesis of 21-nt reproductive phasiRNAs in pre-meiotic anthers (Pokhrel et al., 2021). In grass, however, these 21-nt phasiRNAs direct target mRNA cleavage in male germ cells, suggesting a role in anther development (Pokhrel et al., 2021). In non-model plants, fewer studies investigate the sRNAs roles other than miRNAs and phasiRNAs. Hairpin-derived siRNAs (hp-siRNAs), a considerable component of the sRNA population in plants, have been emerging as an important regulator in certain biological processes. For example, hp-siR227s from *MdHPL277* in apple are induced by the pathogen *Alternaria alternata* infection, contributing to *A. alternata* leaf spot resistance (Zhang et al., 2018).

Strigolactone (SL) is a plant hormone involved in shoot branching and other biological processes (Gomez-Roldan et al., 2008). In rice and *Arabidopsis*, the SL perception and signaling pathway is well known (Hamiaux et al., 2012; Yao et al., 2016). The α/β -fold hydrolase DWARF14 (D14), is an SL receptor that recognizes SL and hydrolyses SL (Hamiaux et al., 2012; Yao et al., 2016). The combination of D14 with the released D-ring from SL recruits the SCF (SKP1, CULLIN, and F-BOX) complex. The SCF complex mediates degradation of SUPPRESSOR OF MAX2 1-LIKE 6/7/8 (SMXL, D53 in rice) via the ubiquitin 26S proteasome system (Yao et al., 2016), leading to

derepression of related transcription factors (such as SPLs) and the activation of SL-elicited responses (Wang et al., 2020; Xie et al., 2020). *d14* mutants in rice and *Arabidopsis* promote shoot branching and alter plant architecture (Arite et al., 2009; Seto et al., 2019). Post-transcriptional gene silencing (PTGS) also regulates plant architecture. For example, miR156 mediates *OsSPL14* cleavage (Jiao et al., 2010; Miura et al., 2010), which functions in parallel with SL signaling (Song et al., 2017). However, to date, there is few research on the role of PTGS in SL perception and signaling.

Compared with *Arabidopsis*, some biological processes during the flower development of longan and other Sapindaceae fruit trees are species-specific, such as inflorescence architecture formation and flower sex differentiation. To unveil the post-transcriptional regulation mechanism of longan flower development, we performed comprehensive analyses of miRNA/phasiRNA/hp-siRNA and their target genes.

2. Materials and methods

2.1. Plant materials

Three 10-year-old 'Shixia' longan, one of the main cultivars in China, were used for this study. Trees were planted in the South China Agricultural University orchard (Guangzhou, China, longitude and latitude are 113.4, 23.2, respectively). Different tissues, including flower buds in stage 1 ($1.0 < \text{diameter} \leq 2.0$ mm, FB-S1), stage 2 ($2.0 < \text{diameter} \leq 2.5$ mm, FB-S2), stage 3 ($2.5 < \text{diameter} \leq 3.0$ mm, FB-S3), stage 4 (diameter more than 3.0 mm, FB-S4), stage 5 (flower buds that were about to bloom, FB-S5), male flowers (full blooming, MF), female flowers (full blooming, FF), shoots (SH), young leaf (leaves approximately 3 cm long with light green color, YL), old leaves (dark green and leathery leaves, OL), and roots (root tips with approximately 10 cm in length, RO), were collected for sRNA and degradome sequencing. All samples with similar growing conditions were collected from the three trees and quickly frozen in liquid nitrogen and stored at -80 °C.

2.2. Small RNA and degradome sequencing

Total RNA was extracted using RNAiso Plus (for RNA extraction, TaKaRa, Code No. 9108) and Fruit-mate (for polysaccharide/polyphenol removal, TaKaRa, Code No. 9192) kits, according to the product manual. A total of 5 μg total RNAs with an RNA Integrity Number (RIN) higher than 7.5 were used for sRNA and degradome library construction. In total, 32 sRNA libraries were constructed and sequenced on an Illumina HiSeq 2500 platform at Novogene (Beijing, China), following standard operating procedures. A total of 50 μg of total RNA from reproductive tissues (FB-S1 to S5, MF, and FF) and vegetative tissues (SH, YL, OL, and RO) were equally mixed and used to construct degradome libraries, respectively, and sequenced on an Illumina HiSeq 2500 platform at Lianchuan Biological Technology Co., Ltd. (Hangzhou, China) following standard operating procedure. All sRNA and degradome raw data generated in this study have been deposited into CNGB Sequence Archive (CNSA, <https://db.cngb.org/cnsa/>) of China National GeneBank DataBase (CNGBdb) with accession number CNP0002481.

2.3. Data preprocessing

Raw data were preprocessed as previously published (Feng et al., 2019; Chen et al., 2021). In brief, adaptor sequences, short reads, and low-quality reads, were removed from sequencing data. Then, non-coding RNAs (rRNA, snoRNA and tRNA) and tags from the chloroplast and mitochondrial genomes were removed by mapping against Rfam V13.0 (<https://rfam.org/>) (Kalvari et al., 2018) and The Plant Organelles Database 3 (<http://podb.nibb.ac.jp/Organellome/podb3/search.php>) (Mano et al., 2014), respectively. Preprocessed reads were mapped to the 'Shixia' longan genome (https://www.ncbi.nlm.nih.gov/assembly/GCA_020457875.1/) by bowtie (Langmead, 2010), allowing one mismatch within the alignment for further analyses.

2.4. miRNA and PHAS loci identification

The procedure and detailed parameters of miRNA annotation and PHAS loci identification have been described previously (Feng et al., 2019; Chen et al., 2021). In brief, a MIR locus should achieve the following criteria: (1) the space size between mature miRNA and miRNA star (miRNA*) should be between 5-nt and 300-nt, (2) the mature miRNA should be 20-nt to 22-nt in length, (3) sRNA with more than 20 hits in the genome were filtered as they are likely from repeated sequences, (4) the miRNA and miRNA* abundance should be more than 75% of total reads from MIR locus, and (5) 90% of the mapped reads should be located on the sense strand of the precursor. Each new MIR locus was checked manually according to the latest established standards to obtain a high confidence miRNA identification (Axtell and Meyers, 2018). Known miRNAs were named according to homology, while "miRN" was used as a prefix for nominating novel miRNAs. In a certain novel MIR locus, miRNA* with notable abundance (30% higher than the sum of miRNA and miRNA*) were considered as functional small RNAs and remained for subsequent analysis.

PHAS loci identification was based on *P*-value and phasing score (Xia et al., 2013). A PHAS locus must meet the following requirements: (1) the most abundant siRNAs should be either 21-nt or 24-nt long, (2) the in-phase siRNAs abundance should be more than 30%, (3) each PHAS locus should be more than 100 bp long, (4) the *P*-value should be less than 0.001 while phasing score should be more than 10. And 400 bp flanking sequences (200 bp upstream and 200 bp downstream) plus the sequence of each PHAS locus were used to identify trigger miRNA, and the penalty score of the alignment between trigger miRNAs and PHAS loci should be no more than 5.

2.5. Hairpin loci identification

An in-house pipeline was developed to identify hairpin loci in the longan genome, followed by a strict manual check. First, sRNA clean reads were mapped to the longan genome using bowtie (Langmead, 2010) with modified parameters: (1) sRNA with no more than 50 hits in the genome were considered, and (2) one mismatch was allowed (-m 50 -v 1). Second, the hcsiRNAMinerCLI module from TBtools (Chen et al., 2020, 2021) was adapted to detect sRNA generating loci with modified parameters: (1) sRNA loci with an interval of 500-bp were considered as separate locus (--minRegionGap 500), (2) all 20-nt to 24-nt sRNA were considered (--targetLens 20, 21, 22, 23, 24), (3) the abundance ratio of 20-nt to 24-nt sRNA should be more than 90% (--minRepeatRatio 0.9). Third, a manual check was conducted using IGV-sRNA (Chen et al., 2021) for each hairpin loci to ensure that sRNA was mapped

into both strands, the whole locus could be folded into a long hairpin secondary structure, and the sRNA distribution in 5' arm of hairpin loci displayed similar pattern as the 3' arm, forming an "symmetric" feature.

2.6. Identification of target genes for miRNA, phasiRNA and hairpin loci

Degradome data were used to identify target genes for miRNA and phasiRNA via CleaveLand 4.0 (Brousse et al., 2014). Target genes were classified into five categories (0–4). Target transcripts with confident level of category 0–2 and alignment penalty score no more than 5 in one library were considered credible miRNA cleave sites.

To identify downstream target genes of hairpin loci, we used the sequences of each hairpin locus as blastn queries (Camacho et al., 2009) (-evalue 1e-5) against longan coding sequences. The resultant transcripts were annotated as potential target genes of hairpin sRNAs unless they meet at least one of the following requirements: (1) the identity of target genes is more than or equal to the average, (2) the alignment length of target genes is more than or equal to the average.

2.7. qRT-PCR analysis

To determine the *DID14* expression, the RNA samples used in the small RNA library construction were used to perform qRT-PCR analysis. HiScript II QRT SuperMix (Vazyme) and GoTaq qPCR Master Mix (Promega) were used in reverse transcription and qPCR, respectively, following the manufacturer's instructions. Two pairs of primers flanking the target sites of miRN15 and hp-siRNAs from *HPL-056* were designed. The primers flanking miRN15 target site sequence were forward 5'-GATAACTATCTTGTACTIONGGTCAT-3' and reverse 5'-AAGGTCATAGAAAACGATACG-3'. For hp-siRNA target site, 5'-ATGCCAGAAGCCATACAA-3' forward and 5'-TCACTTGACTGAGGACATC-3' reverse primers were used. The *Actin* gene was used as a reference gene in the qRT-PCR assay, following kit instructions (GoTaq® qPCR Master Mix, A6001, Promega) with Bio-Rad/CFX Touch real-time PCR system. Expression levels were calculated as the mean of relative fold changes of three biological replicates.

3. Results

3.1. miRNAs directed post-transcriptional regulation in longan flower development

To dissect the post-transcriptional regulation of longan flower development, seven reproductive tissues (including flower buds in five different developmental stages, and mature male and female flowers) and four vegetative tissues (including shoots, young leaves, mature leaves, and roots) were used in small RNA sequencing. In contrast, mixed reproductive tissues and mixed vegetative tissues were used in degradome analyses (Fig. 1, a). sRNA and degradome data analysis by canonical processing procedure showed more than 1.4 million unique, clean reads were obtained for each library. Furthermore, more than 70% of clean reads were mapped to the latest longan genome (Table S1), suggesting our data were of high quality.

In total, 143 known miRNAs belonging to 40 miRNA families and 52 novel miRNAs derived from 44 novel *MIR* loci were identified (Table S2). Some miRNA family members showed tissue preferential expression patterns.

Compared with other members of the miR156 family, miR156a was dominantly expressed in longan flower buds, miR156c preferred to accumulate in leaves, and miR156f was expressed mainly in roots. miR172c was highly expressed in reproductive tissues while miR172a/b ruled in vegetative tissues (Table S2). Some miRNA family members shared similar expression patterns, such as all miR2275 members were reproductive tissue-specific and highly expressed in early developmental stages (Table S2). Among all miRNAs, 27 were of higher expression (foldchange > 2, RP10M > 10 in more than 1 library) in reproductive tissues (Fig. 1, b), which might play crucial roles in longan flower development. miR156a is highly expressed in the early flower bud stage and decreases with the development of flower buds. At the same time, miR172c accumulates over time with increasing age of flower buds, suggesting miR156a and miR172c are likely involved in the juvenile-adult phase transition of longan flower, consistent with previous reports (Wu et al., 2009) (Table S2). miR2118 aroused earlier in flower bud stage 1, while miR2275 was highly expressed around stage 3, following the expression pattern of miR2118 and miR2275 in the grass, indicating that they might have a similar function in reproductive development. Besides conserved miRNAs, eight novel miRNAs were also predominantly expressed in reproductive tissues, such as miRN15.

Plant miRNAs serve as post-transcriptional regulation factors via direct slicing on their target genes. Degradome sequencing was performed using mixed reproductive and vegetative tissues to obtain informative regulatory networks of longan miRNAs. After analyses, 262 genes were identified as targets of 51 miRNAs with strict criteria (the penalty score should be ≤ 5 , and the confidence category should ≤ 2 in at least one library) (Table S3). As expected, many conserved miRNA-target pathways were confirmed, for example, miR156-*SPL*, miR159/miR828/miR858-*MYB*, miR160/miR167-*ARF*, miR164-*NAC*, miR172-*AP2*, miR396-*GRF*, miR397-*Laccase coding genes*, and miR482-*disease resistance genes*. Besides, 52 transcripts were targeted by 18 novel miRNAs, which might be unique regulatory pathways in longan (Table S3). Comparison of degradome signal level of each target gene (normalized by RP10M) between reproductive and vegetative tissues showed 56 target genes were notably repressed in reproductive tissues (red dots in Fig. 1, c), while 53 targets were repressed greatly in vegetative tissues (blue dots in Fig. 1, c), suggesting miRNA-directed post-transcriptional regulations differ between reproductive and vegetative tissues. This could be possibly due to the preferential accumulation of related miRNAs in different tissues. For example, miR172c was mainly expressed in reproductive tissues, leading to its target gene, *Dil.14g006820*, sliced at a higher degree. Higher expression of the novel miRNA, miRN15, in reproductive tissues caused the specific cleavage of *Dil.06g005400* (Fig. 1, d). These reproductive tissue-specific miRNAs may lead to unique or preferential regulations essential for flower development in longan.

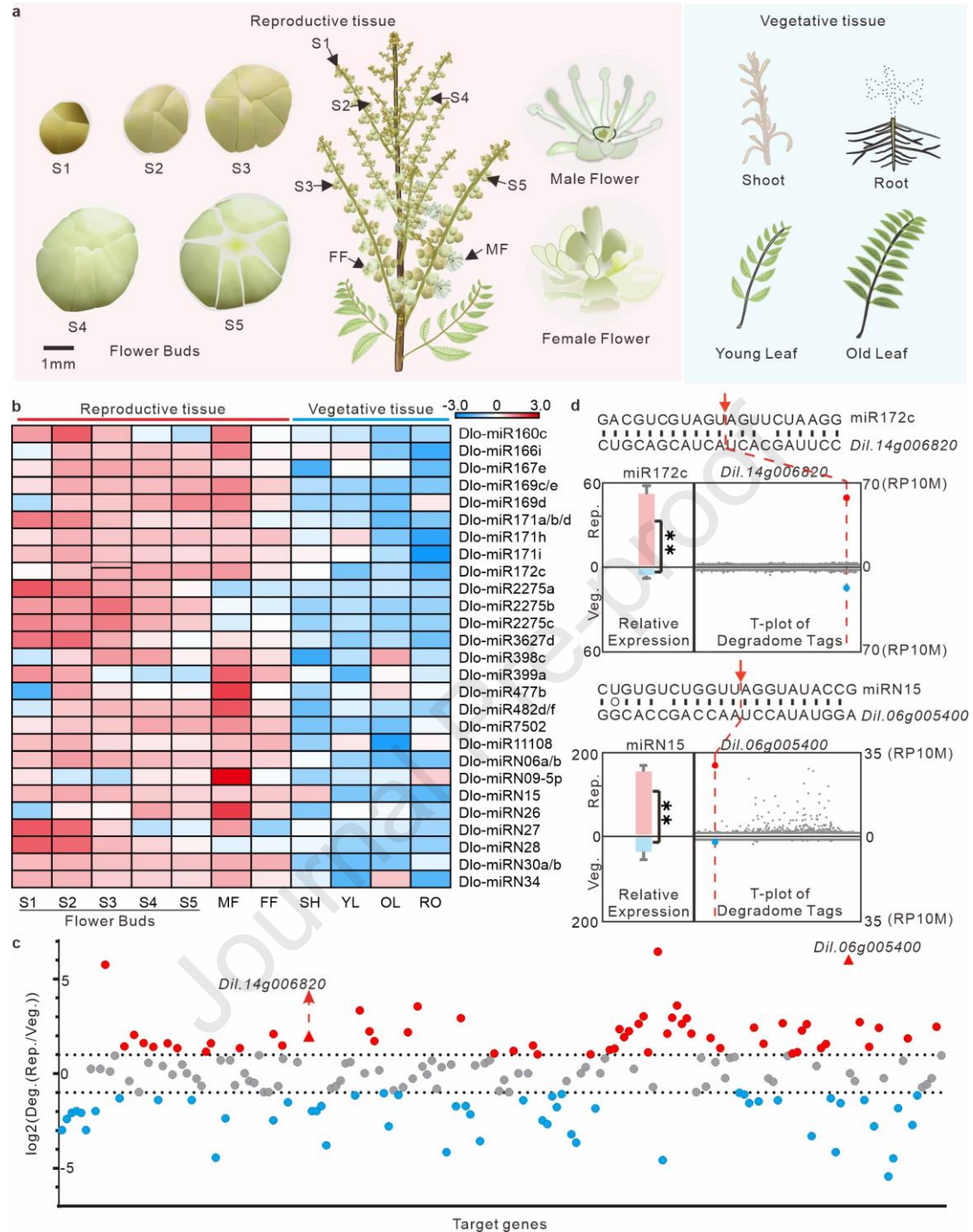


Fig. 1 miRNA directed regulatory pathway that was involved in longan reproductive tissues

(a) Schematic representation of reproductive and vegetative tissues used in sRNA and degradome sequencing. Flower buds stage 1 ($1.0 < \text{diameter} \leq 2.0$ mm, S1), stage 2 ($2.0 < \text{diameter} \leq 2.5$ mm, S2), stage 3 ($2.5 < \text{diameter} \leq 3.0$ mm, S3), stage 4 (diameter more than 3.0 mm, S4), stage 5 (flower buds that were about to bloom, S5), male flowers (full blooming, MF), female flowers (full blooming, FF), shoots (SH), young leaf (leaves approximately 3 cm long with light green color, YL), old leaves (dark green and leathery leaves, OL), and roots (root tips with approximately 10 cm in length, RO) (b) Expression of miRNAs that predominantly expressed in reproductive tissues. S1-S5: Stage 1-Stage 5 of flower buds, MF: male flower, FF: female flower, SH: shoot, YL: young leaf, OL: old leaf, RO: root. The color bar at the right top side of the panel indicated the relative expression level of miRNAs in different tissues (c) Degradome signal level of miRNA target genes between reproductive and vegetative tissues. Degradome signal level was calculated by log₂ normalized degradome reads (Reads Per 10 Million, RP10M) in reproductive versus vegetative tissues. Red and blue dots represented target genes that were highly repressed in reproductive and vegetative tissues respectively. (d) miR172c and miRN15 regulated *Dil.14g006820* and *Dil.06g005400* in reproductive tissues. The expression level of miRNAs was showed as the average value of reproductive and vegetative tissues. T-plots of target genes were drawn based on degradome data. Red dotted lines and red arrows indicated the cleavage sites of each miRNA. Both sRNA-seq and degradome reads were normalized as RP10M.

3.2. PhasiRNA-directed post-transcriptional regulation in longan flower development

PhasiRNAs are another class of sRNA that regulate plant development and stress defense mainly via PTGS. Using previously published methods, 88 21-nt-*PHAS* and 17 24-nt-*PHAS* loci were identified (each locus's maximum region phasing score should be > 10 in at least one library). miR390 mediated "two-hit" model generated phasiRNAs from two *TAS3*-like loci, while all 24-nt-*PHAS* loci were triggered by miR2275 in longan (Table S4). These two pathways are conserved in land plants and angiosperm, respectively (Xia et al., 2017, 2019). Besides, miR393, miR482, miR828, miR3954, miRN15 were also capable of triggering the biogenesis of phasiRNAs in longan. In addition, we cannot identify miRNA triggers for 52 *PHAS* loci, ten of which were annotated as pentatricopeptide repeat-containing protein (PPR) (Table S4). After calculating the abundance of all siRNAs derived from each *PHAS* loci, we found 22 21-nt-*PHAS* loci and all 24-nt-*PHAS* loci preferentially produced phasiRNAs in reproductive tissues (Fig. 2, a), indicating these *PHAS* loci were probably involved in longan flower development. All 24-nt-*PHAS* loci produced phasiRNAs at the early stage of flower development, concomitant with the expression pattern of their trigger, miR2275 (Fig. 1, b; Fig. 2, a). Similarly, both *PHAS-036* and its trigger, miRN15, showed preferential expression patterns in reproductive tissues (Fig. 1, b; Fig. 2, a, b). miR3954a/b was highly expressed in longan leaves (Table S2), *PHAS-033* and *PHAS-034*, both triggered by miR3954, showed the similar expression pattern as miR3954 (Table S4), but phasiRNAs from *PHAS-035* that was also triggered by miR3954 were specifically accumulated in reproductive tissues (Fig. 2, a b). These results indicated that phasiRNA expression pattern was affected by the expression of its trigger miRNAs and their targeted *PHAS* loci. In addition, some *PHAS* loci showed different expression between male flower and female flower, such as *PHAS-008* and *PHAS-023* targeted by miR482 (Table S4; Fig. 2, c), suggesting these *PHAS* loci might be involved in male or female organ development.

To examine the post-transcriptional roles of longan phasiRNAs, the top 30 most abundant phasiRNAs from each *PHAS* locus were obtained and their target genes were identified using combined degradome data from reproductive and vegetative tissues. These phasiRNAs were termed by the ID of their cognate *PHAS* loci and their abundance rank, e.g., phasiR-013-14, indicates the 14th abundant phasiRNA from *PHAS-013*. As a result, 3 162 genes were identified under the potential regulation of 1 436 phasiRNAs from 88 21-nt-*PHAS* loci (Table S5). 941 and 477 genes were identified as confidential targets (penalty score ≤ 5 and the confidence category ≤ 2) in reproductive and vegetative tissues, respectively (Table S5). miR390 triggered two *TAS3* loci producing tasiARFs, which *in trans* regulated *ARF2A* (*Dil.12g014490*), *ARF3* (*Dil.07g016180*), and *ARF4* (*Dil.13g006460*) in longan (Table S5). PhasiRNAs triggered by miR482 and miR828 were also confirmed as regulators of nucleotide binding-leucine rich repeat (NB-LRR) protein-coding genes and *MYB*, involved in disease resistance and anthocyanin biogenesis, respectively (Table S5), as previous studies reported (Zhai et al., 2011). PhasiRNAs derived from *PHAS-034* and *PHAS-035* triggered by miR3954 were suggested to regulate *NAC* (*NAM*, *ATAF1/2*, and *CUC2*) genes and *PPR* genes respectively (Table S5). Intriguingly, reproductive tissues specific phasiRNAs from *PHAS-036* (annotated as SL receptor-like gene, Fig. 2, a b) triggered by miRN015 *in cis* regulated two *D14-like* genes (*Dil.06g005400*, *Dil.09g009750*) in longan (Table S5). This regulatory pathway is a novel one that has not been reported before, which might be involved in suppressing SL signal transduction in longan reproductive tissues.

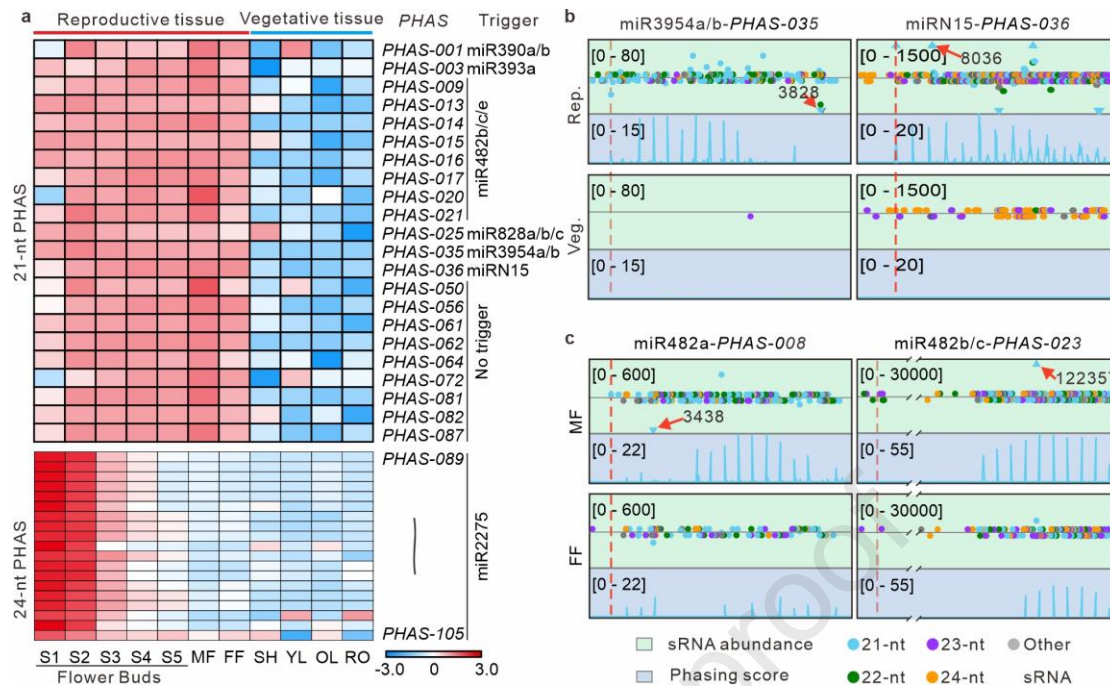


Fig. 2 PhasiRNA-directed regulatory pathways that were involved in longan reproductive tissues

(a) Expression of phasiRNAs from *PHAS* loci that predominantly expressed in reproductive tissues. The color bar at the right bottom of the panel showed the relative expression level of phasiRNAs in different tissues (b) miR3954 and miRN15 regulated *PHAS-035* and *PHAS-036*, respectively, and triggered phasiRNA biogenesis specifically in reproductive tissues. The original data of Rep. and Veg. for plotting were from library FB-S3-R2 and YL-R2. IGV-sRNA was used in data plotting. The y-axis scales are showed at top left corner of each track. Dots in different colors represent sRNA with different length. Red dotted lines indicate the cleavage sites of trigger miRNAs. Triangle dots represent sRNAs whose abundance exceeds the range of Y coordinates. (c) miR482 targeted *PHAS-008* and *PHAS-023* and triggered phasiRNA biogenesis in both male and female flower, with higher expression level in male flower. Plotting data of MF and FF were from library MF-R3 and FF-R3. MF (full blooming male flowers), FF (full blooming female flowers).

3.3. Functional specialization of the miR482-*PHAS* module in longan flower development

miR482 and miR2118 are members of the miR482/2118 superfamily that originated from gymnosperm. miR482 and miR2118 mainly targets *NB-LRRs* in eudicots and long non-coding RNAs in grasses. Also, they trigger phasiRNAs biogenesis, which are involved in plant immune and reproductive development (Zhai et al., 2011; Komiya et al., 2014; Zhang et al., 2021). miR482-type mature sequences beginning with “UC” have a 2-nt shift forward compared with miR2118-type, which started with “UU” (Zhang et al., 2021). Six *MIR482* loci, encoding four different mature sequences, were identified in longan. Among them, miR482b/c/e were miR482-type mature sequences, while miR482a/d/f were miR2118-type. miR482b/c and miR482d/f were predominantly accumulated in reproductive tissues (Fig. 3, a). Twenty *PHAS* loci triggered by the miR482 family were identified in longan (Table S5; Fig. 3, b). The *PHAS* loci could be categorized into two groups based on the expression pattern of phasiRNAs (Fig. 3, b). Notably, *PHAS* loci belonging to group I displayed a clear preferential expression in reproductive tissues, while *PHAS* loci in group II were ubiquitous in both reproductive and vegetative tissues (Fig. 3, b; Table S4).

Next, we explored miR482-*PHAS* module potential biological function by analyzing their downstream genes. *PHAS* loci preferentially expressed by reproductive tissues are mostly involved in biological processes related to development. In contrast, most of the genes regulated by the second group of *PHAS* loci are associated with disease resistance (Fig. 3, b; Table S5). These data suggested that the miR482-*PHAS* module might be functionally specialized in longan flower tissues. In particular, miR482 targeted a non-coding transcript *PHAS-012* and triggered

the biogenesis of phasiRNAs. The top two abundant phasiRNAs (phasiR-012-01/02) targeted four genes with higher confidence levels (category = 0 and penalty score ≤ 3.5 ; Fig. 3, c, Table S5) in reproductive tissues, all of which were annotated as squalene synthase coding genes. Squalene is a triterpene, a biochemical intermediate, a precursor for the synthesis of β -amyrin and saponins, important secondary metabolites in the Sapindaceae family (Thimmappa et al., 2014). These results indicated that the miR482-*PHAS* module had probably adapted expanding functions in certain biological processes in specific plant lineages.

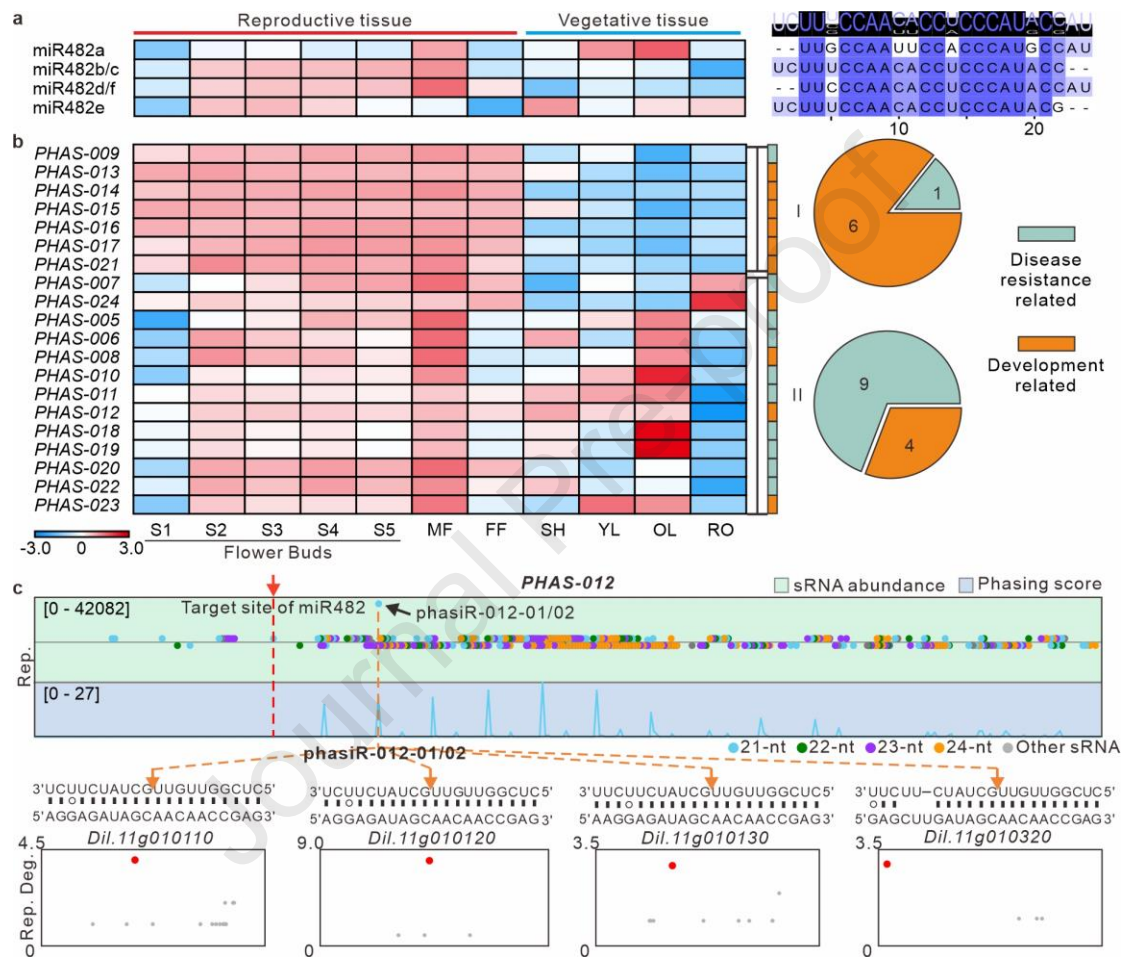


Fig. 3 Expanding function of miR482-*PHAS* in longan flower development

(a) Expression of different members of miR482 in different tissues. Multiple sequence alignment of miR482 mature sequences was applied by Clustal Omega (<https://www.ebi.ac.uk/Tools/msa/clustalo/>) and viewed in Jalview (V2.11). (b) PhasiRNA expression of *PHAS* loci targeted by miR482 in different tissues. Pie charts showed the function proportion of *PHAS* loci in each class. The color bar at the left bottom of the panel displayed the sRNA expression level in different tissues (c) miR482 triggered the biogenesis of phasiRNA from *PHAS-012* and two resultant phasiRNAs regulated four squalene synthase coding genes. The original data of Rep. for plotting were from library FB-S4-R2. The red dotted line and red arrow indicated the cleavage site of miR482 while orange arrows showed the cleavage site of phasiR-012-01/02.

3.4. siRNAs derived from transcripts containing hairpin structure regulated downstream genes in cis or trans

While analyzing sRNA data, several sRNA loci containing two sRNA enriched blocks drew our attention due to their symmetric sRNAs distribution in the Integrative Genomics Viewer (Fig. 4, a; Fig. S1). Further analysis showed that these sRNA loci harbored a secondary long stem-loop (hairpin-like) structure. The sRNA distribution in the 5'

arm of a hairpin loci (*HPL*) showed an extreme similarity with the 3' arm, contributing to the "symmetric" feature (Fig. 4, a). As aforementioned, siRNAs from hairpin structures have been reported as post-transcriptional regulators in plant development (Borges and Martienssen, 2015; Zhang et al., 2018). Hence, we developed a genome-wide in-house pipeline to identify *HPLs* from the genome of longan. In total, 120 *HPLs*, between 563-nt to 14 531-nt in length were identified (Table S6). The proportion of hp-siRNA (6.48% of all sRNAs in all libraries) was larger than miRNA (5.11%) and phasiRNA (5.15%), indicating hp-siRNAs were likely another major subgroup of siRNAs involved in post-transcriptional regulation in longan (Fig. 4, b).

Unlike miRNAs and phasiRNAs, most of hp-siRNAs (111 out of 120 loci) showed preferential expression in reproductive tissues (Fig. 4, c; Table S6), suggesting their roles in reproductive development. Small RNAs' function and action mode mainly depend on their length and association with ARGONAUTE (AGO) proteins. Small RNAs with a length of about 21-nt (20-nt to 22-nt, short sRNA) associate with the AGO1 or AGO2 clades to direct PTGS, while sRNAs of 24-nt (long sRNA) interact with the AGO4 clade to mediate TGS (Mallory and Vaucheret, 2010). Thus, we calculated the length distribution of sRNAs of each *HPL* from all libraries. Consequently, 79 out of 120 *HPL* mainly produced short 20–22-nt sRNAs. However, the length distribution of sRNA from a certain *HPL* varied in different tissues. There were 102 out of 120 loci mainly producing short sRNAs in male flowers, while only 66 loci generating short sRNAs in female flowers (Table S6). Almost in all loci (119/120), the proportion of short sRNA that played main roles in PTGS was higher in male flower (red line in Fig. 4, d) than in female flower (black line in Fig. 4, d), which might be due to different activities of DCLs between male and female flower. These data suggested that hp-siRNAs directed PTGS might be involved in reproductive development and of different effects between male and female flowers.

In contrast to the erratic phasiRNA biogenesis, hp-siRNAs from *HPL* could be processed by multiple DCLs, resulting in an unstable expression pattern of hp-siRNAs. Thus, we used hp-siRNA-generating regions of each *HPL* as queries to identify their potential target genes. As a result, 595 genes were identified as downstream targets. Some *HPLs* overlapped with coding genes could potentially regulate their homologous genes or other unrelated downstream genes (Table S7) involved in various biological processes. Such as *HPL-024*, *HPL-025*, and *HPL-029* could co-regulate 14 *NAC* genes, and *HPL-030*, *HPL-035*, *HPL-041* regulate *ARF7* and *ARF13*. As most hp-siRNAs from a certain region could mediate post-transcriptional slicing on their target genes, multiple significant degradome signals could be observed in the target transcripts. Notably, *HPL-044* and *HPL-063* were specifically expressed in reproductive tissues (Fig. 4, e; Table S6), the hp-siRNAs from which mediated multiple cuts in *Dil.05g012340* and *Dil.12g019370* specifically in reproductive tissues as well (Fig. 4, e), indicating hp-siRNAs from *HPL-044* and *HPL-063* mediated PTGS occurred specifically in reproductive tissues. *HPL-044* regulated nine F-box protein-coding genes (including *Dil.05g012340*, Fig. 4, e, Table S7), which were components of SCF (SPK-cullin-F-box) E3 ubiquitin ligase complexes that could be involved in the ubiquitination of protein degradation pathway. *HPL-063* targeted four genes encoding Cyclic nucleotide-gated ion channel proteins (including *Dil.12g019370*, Fig. 4, e, Table S7), which could be involved in pollen development in plants (Kaplan et al., 2007). Our data provided new insights that hp-siRNAs, besides well-studied miRNA and phasiRNA, were another large population of sRNAs that can mediate PTGS in reproductive development in longan.

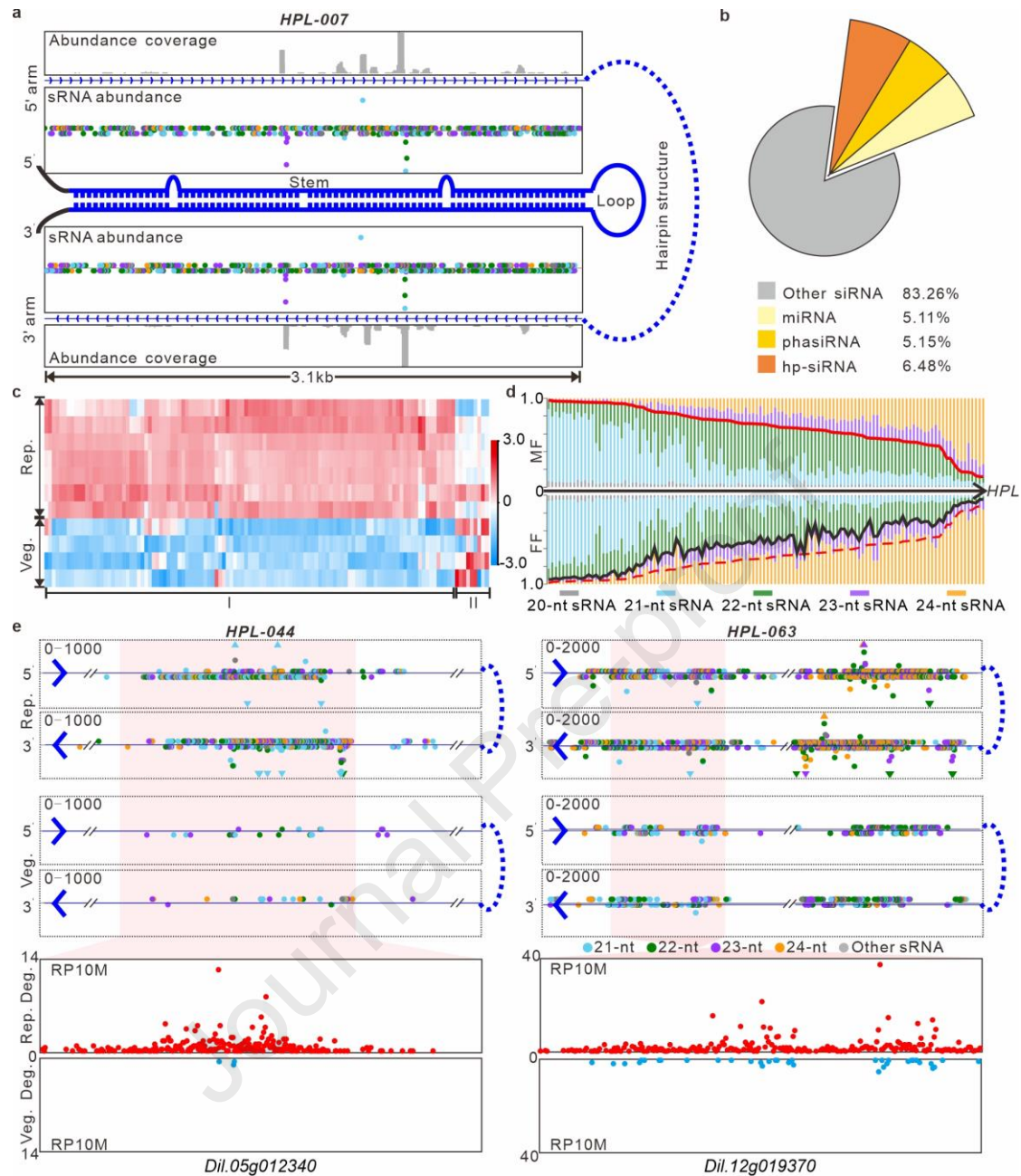


Fig. 4 The profile of hairpin loci in longan

(a) Schematic representation of sRNA production from a hairpin locus. (b) The abundance proportion of miRNA, phasiRNA and hp-siRNA in longan. The population of each sRNA class was calculated by the average value of all sRNA libraries. (c) sRNA abundance of all hairpin loci in reproductive tissues (The tissues were S1, S2, S3, S4, S5, MF and FF from top to bottom) and vegetative tissues (The tissues were SH, YL, OL and RO from top to bottom). The color bar at the right of the panel indicated the sRNA expression level in different tissues. (d) Length distribution of hp-siRNAs from each hairpin locus in male and female flower. The red line indicated the proportion of short hp-siRNAs (20-nt to 22-nt) of each *HPL* in male flower, while the black line showed the proportion of short hp-siRNAs of each *HPL* in female flower. The red dotted line was the reflective image of the red line. (e) hp-siRNAs from *HPL-044* and *HPL-063* regulated *Dil.05g012340* and *Dil.12g019370*. The original data of Rep. and Veg. for plotting were from library FB-S4-R2 and OL-R2. The pink shadow indicated the hp-siRNA region that could regulate downstream target genes.

3.5. miRN15 cooperated with *HPL-056* and *HPL-068* to regulate *SL* receptor gene *D14*

Strigolactone acts as an important phytohormone regulating plant development and response to environmental stimuli. Few works report siRNA directly involved in the SL signaling transduction pathway. In our results, a novel miRNA, miRN15 and hp-siRNAs from *HPL-056* and *HPL-068* targeted SL receptor gene *DID14*

(*Dil.06g005400*) and triggered secondary siRNA from *DID14* (Tables S3 and S7). miRN15 was highly expressed in reproductive and shoot tissues and almost absent in leaves and roots (Fig. 5, a; Table S2). Hp-siRNAs from *HPL-056* showed a similar expression pattern as miRN15, except for old leaves, showing moderate accumulation (Fig. 5, b; Table S6). miRN15 was 22-nt in length derived from a duplex with an asymmetric mismatch (bulge, Fig. 5, c), and it triggered the biogenesis of phasiRNAs starting from its cleavage site in the first exon of *Dil.06g005400* (red dot line in Fig. 5, e). The secondary phasiRNAs (~21 nt) biogenesis was detected in all reproductive tissues but absent in shoots, leaves, and roots (Fig. 2, a; Fig. S2), indicating the miRN15-*DID14*-phasiRNA module was involved in SL signal transduction specifically in reproductive tissues. It is puzzling why miRN15 was accumulated in the shoots where phasiRNAs from *Dil.06g005400* were absent. Potential regulators might have blocked the miRN15 directed slicing on *Dil.06g005400* in longan shoot.

Simultaneously, a region of 262-nt in *HPL-056* (the same region could be found in *HPL-068*), where abundant hp-siRNAs were accumulated, showed 76.34% sequence similarity with the second exon of *Dil.06g005400* (Fig. 5, d; Table S7), indicating that this group of hp-siRNAs from *HPL-056* and *HPL-068* likely regulate *DID14* via PTGS (Fig. 5, d, e, pink shadow). As 34% of hp-siRNAs from *HPL-056* were in the length of 22-nt (Table S6), we next checked if hp-siRNAs from *HPL-056* could trigger the secondary siRNA biogenesis. To exclude the influence from phasiRNAs triggered by miRN15, sRNA data from old leaf and young leaf were used, since miRN15 was absent in both old leaf and young leaf while hp-siRNAs from *HPL-056* were moderately expressed in old leaf and almost undetectable in young leaf (Fig. 5, a, b). As a result, compared with the first exon that generated 24-nt noise siRNA, 21-nt secondary siRNAs were accumulated from the second exon in old leaves and shoots (Fig. 5, e). These secondary siRNAs were not processed in phase and were mainly expressed in a single site (red arrow in Fig. 5, e). In contrast, these secondary siRNAs were almost gone in young leaf and root, especially in the site marked by an orange arrow (Fig. 5, e). This result was in line with the expression pattern of hp-siRNAs from *HPL-056* (Fig. 5, b), suggesting that hp-siRNAs from *HPL-056* targeted *Dil.06g005400* and triggered secondary siRNA biogenesis. We also checked the expression of *DID14* (*Dil.06g005400*) during flower development, qRT-PCR primers with the consideration of the target sites of miRN15 and hp-siRNAs from *HPL-056* were designed for the test. A similar expression pattern of *DID14* was detected (Fig. S3). *DID14* expression was increased during the flower bud development while miRN15 was decreased (Fig. 5, a; Fig. S3), suggesting miRN15 might be the dominant regulator in the process of flower development.

Our data demonstrated that SL signal receptor gene *D14* was under post-transcriptional regulation of a novel *MIR* and two *HPL* loci (Fig. 5, c, d, e), suggesting that *DID14* may be regulated at three different levels in different tissues. *Dil.06g005400* was suppressed in all reproductive tissues by miRN15 and hp-siRNAs, triggered abundant secondary siRNAs, most of which were in phase, and rendered strong repression of *DID14* and its homologs (level I in Fig. 5, e). In old leaf and shoot, only hp-siRNAs and moderated secondary siRNAs triggered by them were in charge of the regulation of *DID14* (level II). In young leaves and roots where the miRN15 and hp-siRNAs were absent, *DID14* was not underregulated by PTGS (level III). Different sRNAs generating from various pathways were involved in the regulation of *DID14*, providing multiple PTGS layers to fine-tune the expression of *DID14* and subsequent precise modulation of SL perception and signaling.

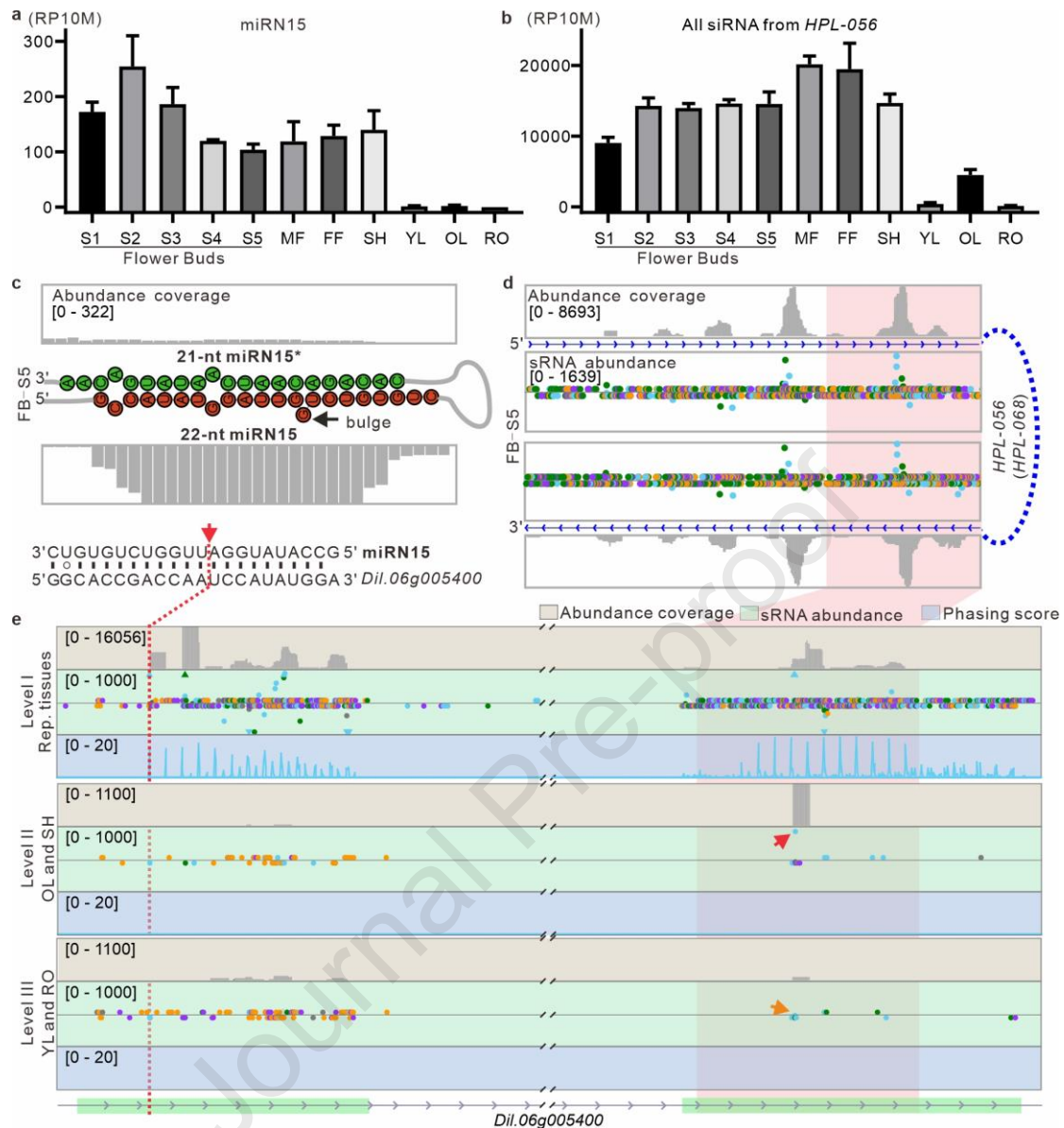


Fig. 5 miRN15 and HPL-056 co-regulated *DID14* in different tissues

(a) Expression of miRN15 in different tissues. The value was normalized as RP10M. (b) Expression of *HPL-056* sRNAs in different tissues. (c) Schema showing the secondary structure and the sRNA abundance coverage along the precursor of miRN15. The original data were from FB-S5-R2 (Second biological replication for flower buds to bloom). The red arrow indicates the cleavage site of miRN15 on *DID14*. (d) hp-siRNA production from *HPL-056*. Pink shadow showed the hp-siRNA region that could regulate *DID14*. (e) miRN15 and *HPL-056* co-regulated *DID14* and triggered abundant secondary siRNAs in reproductive tissues (level I). Only *HPL-056* siRNAs regulated *DID14* in old leaf and shoot (level II) and triggered the biogenesis of secondary siRNA (red arrow). Almost no secondary siRNA production on *DID14* in young leaf and root (level III, orange arrow). The original data used for plotting in level I, II, and III, were from FB-S5-R2, OL-R2 (Second biological replication for dark green and leathery leaves) and YL-R2 (Second biological replication for leaves approximately 3 cm long with light green color), respectively.

4. Discussion

Plant small RNAs have been extensively studied in the past two decades. Some, like miRNAs and phasiRNAs, are processed via specific biogenesis pathways by conserved proteins (Achkar et al., 2016; Liu et al., 2020a). At their discovery, miRNAs were thought to be conserved across the plant kingdom. Conserved miRNAs from non-model plants were cloned based on their homologs in model plants; however, after broader analyses, only 22

miRNA families were highly conserved across Tracheophyta species (Chávez Montes et al., 2014). Much more miRNA families were found to be lineage- or species-specific, and with lineage-specific or species-specific functional diversification (Chávez Montes et al., 2014). As for phasiRNAs, miR390-*TAS3* is conserved in land plants (Xia et al., 2017). miR2118-directed phasiRNA pathways emerged in seed plants, although they are absent in some lineages (Pokhrel et al., 2021). MiR2275 and 24-nt phasiRNAs' expression patterns were consistent in all angiosperms (Xia et al., 2019). miR828-*MYB* is conserved in eudicots and some monocots (Liu et al., 2020b). Other lineage-specific phasiRNA pathways involved in specific biological processes, such as the miR1507/miR1510 triggered phasiRNA biogenesis involved in nodule development in soybean (Zhai et al., 2011), and the miRFBX cluster and its resultant phasiRNAs targeted *F-BOX* genes related to the fruit shape of strawberry (Xia et al., 2015) have been identified. *Cuscuta* miR12480 triggers the phasiRNAs biogenesis from *SEOR1* that targeted host genes, facilitating its parasitic activity (Shahid et al., 2018). In addition, conserved miRNA or phasiRNA pathways may adopt new functions in a lineage. For example, miR482-*NBLRR* is involved in disease resistance in angiosperms, while regulating nodule development in soybean (Zhai et al., 2011). miR828-*MYB* is involved in the light signal pathway and wounding response (Shuai et al., 2016). Besides miRNAs and phasiRNAs, hp-siRNA might be a neglected regulator in PTGS, and hairpin RNAs were suggested to be proto-*MIRNAs* in plants; thus, the extant hairpin loci could be newly evolved or "young" regulatory loci (Borges and Martienssen, 2015), suggesting they were non-conserved and might be involved in a specific pathway in a specific species or lineage.

This study profiled sRNA regulatory circuits in the horticulture fruit crop longan. Apart from conserved sRNA-involved pathways, our analyses focused on the novel longan-specific pathways related to flower development. Eighteen novel longan miRNAs targeted 52 transcripts. Besides, the miR482-*PHAS* pathway showed expanded function in longan, including in secondary metabolism, by targeting squalene synthase genes. Most of the identified 120 hairpin loci from all libraries showed a higher hp-siRNAs accumulation in reproductive tissues. Intriguingly, almost in all hairpin loci, the proportion of short (20 nt to 22 nt) hp-siRNAs is higher in male flowers than in female flowers, suggesting their involvement in sexual organ development or flower sex differentiation in longan. In particular, dlo-miRN15 along with *HPL-056* regulated SL receptor gene *D14* were firstly discovered. SL is a plant hormone involved in many different aspects of plant development, including shoot branching, leaf elongation, and anthocyanin biosynthesis in *Arabidopsis* (Wang et al., 2020), plant architecture (tillering) in rice (Miura et al., 2010; Hamiaux et al., 2012), and inflorescence architecture of wheat (Gao et al., 2019). SL binding to the receptor D14 leads to further interaction with SMXLs/D53, mediating the polyubiquitination of the complex and the degradation by the 26S proteasome, which derepress downstream transcriptional factors to activate SL-elicited responses. In *Arabidopsis* and pea, *BRANCHED 1 (BRC1)* acts downstream of SL and control shoot branching (Braun et al., 2012; Wang et al., 2020). In cotton, *BRC1* regulates flowering time and branching by integrating multiple hormone pathways (Sun et al., 2022), and SL-defective tomato plants show severe defects in flowers and fruits (Kohlen et al., 2012), indicating SL involvement in flower development. Our data showed that the sRNA-mediated PTGS on *DID14* in longan was specifically enriched in reproductive tissues, suggesting this pathway might be involved in flower development or inflorescence branching, closely related to fruit set and yield production. Lineage- or species-specific PTGS might be worth more attention, especially in horticultural plants,

because unveiling these pathways may help understand the underlying development mechanism of species-specific features and benefit from their molecular breeding in the future.

Acknowledgments

This work was funded by the National Key Research and Developmental Program of China (Grant No. 2018YFD1000104). This work was also supported by awards from the National Natural Science Foundation of China (Grant Nos. 32002009 and 32072547), The Special Support Program of Guangdong Province (Grant No. 2019TX05N193).

Supplementary materials

Supplementary material associated with this article can be found, in the online version, at doi: 10.1016/j.hpj.2022.

References

- Achkar, N.P., Cambiagno, D.A., Manavella, P.A., 2016. miRNA Biogenesis: A Dynamic Pathway. *Trends Plant Sci*, 21: 1034–1044.
- Arite, T., Umehara, M., Ishikawa, S., Hanada, A., Maekawa, M., Yamaguchi, S., Kyojuka, J., 2009. *D14*, a strigolactone-insensitive mutant of rice, shows an accelerated outgrowth of tillers. *Plant Cell Physiol*, 50: 1416–1424.
- Axtell, M.J., Meyers, B.C., 2018. Revisiting criteria for plant microRNA annotation in the Era of big data. *Plant Cell*, 30: 272–284.
- Borges, F., Martienssen, R.A., 2015. The expanding world of small RNAs in plants. *Nat Rev Mol Cell Biol*, 16: 727–741.
- Braun, N., de Saint Germain, A., Pillot, J.-P., Boutet-Mercey, S., Dalmais, M., Antoniadis, I., Li, X., Maia-Grondard, A., Le Signor, C., Bouteiller, N., 2012. The pea TCP transcription factor PsBRC1 acts downstream of strigolactones to control shoot branching. *Plant Physiol*, 158: 225–238.
- Brousse, C., Liu, Q., Beauclair, L., Deremetz, A., Axtell, M.J., Bouché, N., 2014. A non-canonical plant microRNA target site. *Nucleic Acids Res*, 42: 5270–5279.
- Camacho, C., Coulouris, G., Avagyan, V., Ma, N., Papadopoulos, J., Bealer, K., Madden, T.L., 2009. BLAST+: Architecture and applications. *BMC Bioinformatics*, 10: 1–9.
- Chávez Montes, R.A., De Fátima Rosas-Cárdenas, F., De Paoli, E., Accerbi, M., Rymarquis, L.A., Mahalingam, G., Marsch-Martínez, N., Meyers, B.C., Green, P.J., De Folter, S., 2014. Sample sequencing of vascular plants demonstrates widespread conservation and divergence of microRNAs. *Nat Commun*, 5: 1–15.
- Chen, C., Chen, H., Zhang, Y., Thomas, H.R., Frank, M.H., He, Y., Xia, R., 2020. TBtools: An integrative toolkit developed for interactive analyses of big biological data. *Mol Plant*, 13: 1194–1202.
- Chen, C., Li, J., Feng, J., Liu, B., Feng, L., Yu, X., Li, G., Zhai, J., Meyers, B.C., Xia, R., 2021. sRNAanno—a database repository of uniformly annotated small RNAs in plants. *Hortic Res*, 8: 45.
- Cho, S.H., Coruh, C., Axtell, M.J., 2013. miR156 and miR390 regulate tasiRNA accumulation and developmental timing in *physcomitrella patens*. *Plant Cell*, 24: 4837–4849.
- Feng, L., Xia, R., Liu, Y., 2019. Comprehensive characterization of miRNA and *PHAS* loci in the diploid strawberry (*Fragaria vesca*) genome. *Hortic Plant J*, 5: 255–267.
- Gao, X.Q., Wang, N., Wang, X.L., Zhang, X.S., 2019. Architecture of wheat inflorescence: insights from rice. *Trends Plant Sci*, 24: 802–809.
- Gomez-Roldan, V., Fermas, S., Brewer, P.B., Puech-Pagès, V., Dun, E.A., Pillot, J.P., Letisse, F., Matusova, R., Danoun, S., Portais, J.C., Bouwmeester, H., Bécard, G., Beveridge, C.A., Rameau, C., Rochange, S.F., 2008. Strigolactone inhibition of shoot branching. *Nature*, 455: 189–194.
- Hamiaux, C., Drummond, R.S.M., Janssen, B.J., Ledger, S.E., Cooney, J.M., Newcomb, R.D., Snowden, K.C., 2012. DAD2 is an α/β hydrolase likely to be involved in the perception of the plant branching hormone, strigolactone. *Curr Biol*, 22: 2032–2036.
- Huang, S., Han, D., Wang, J., Guo, D., Li, J., 2021. Floral induction of longan (*Dimocarpus longan*) by Potassium chlorate: application, mechanism, and future perspectives. *Front Plant Sci*, 12: 1–8.

- Jia, T., Wei, D., Meng, S., Allan, A.C., Zeng, L., 2014. Identification of regulatory genes implicated in continuous flowering of longan (*Dimocarpus longan* L.). *PLoS ONE*, 9: 1–24.
- Jiang, P., Lian, B., Liu, C., Fu, Z., Shen, Y., Cheng, Z., Qi, Y., 2020. 21-nt phasiRNAs direct target mRNA cleavage in rice male germ cells. *Nat Commun*, 11: 5191.
- Jiao, Y., Wang, Y., Xue, D., Wang, J., Yan, M., Liu, G., Dong, G., Zeng, D., Lu, Z., Zhu, X., Qian, Q., Li, J., 2010. Regulation of *OsSPL14* by *OsmiR156* defines ideal plant architecture in rice. *Nat Genet*, 42: 541–544.
- Jue, D., Sang, X., Liu, L., Shu, B., Wang, Yicheng, Liu, C., Wang, Yi, Xie, J., Shi, S., 2019. Comprehensive analysis of the longan transcriptome reveals distinct regulatory programs during the floral transition. *BMC Genomics*, 20: 126.
- Kalvari, I., Nawrocki, E.P., Argasinska, J., Quinones-Olvera, N., Finn, R.D., Bateman, A., Petrov, A.I., 2018. Non-Coding RNA analysis using the Rfam Database. *Curr Protoc Bioinforma*, 62: 1–27.
- Kaplan, B., Sherman, T., Fromm, H., 2007. Cyclic nucleotide-gated channels in plants. *FEBS Lett*, 581: 2237–2246.
- Kohlen, W., Charnikhova, T., Lammers, M., Pollina, T., Tóth, P., Haider, I., Pozo, M.J., de Maagd, R.A., Ruyter-Spira, C., Bouwmeester, H.J., 2012. The tomato *CAROTENOID CLEAVAGE DIOXYGENASE 8 (SICCD 8)* regulates rhizosphere signaling, plant architecture and affects reproductive development through strigolactone biosynthesis. *New Phytol*, 196: 535–547.
- Komiya, R., Ohyanagi, H., Niihama, M., Watanabe, T., Nakano, M., Kurata, N., Nonomura, K.I., 2014. Rice germline-specific Argonaute MEL1 protein binds to phasiRNAs generated from more than 700 lincRNAs. *Plant J*, 78: 385–397.
- Langmead, B., 2010. Aligning short sequencing reads with Bowtie. *Curr Protoc Bioinforma*, 32: 11.7.1–11.7.14.
- Lee, Y.C., Chang, J.C., 2019. Leafless inflorescence produces more female flowers and fruit yield than leafy inflorescence in ‘yu her pau’ litchi. *Hort Science*, 54: 487–491.
- Li, P., Su, T., Zhang, D., Wang, W., Xin, X., Yu, Y., Zhao, X., Yu, S., Zhang, F., 2021. Genome-wide analysis of changes in miRNA and target gene expression reveals key roles in heterosis for Chinese cabbage biomass. *Hortic Res*, 8: 1–15.
- Li, Y., Meng, X.W., Ma, Z.H., Liu, M.J., Zhao J., 2022. Identification and expression analysis of microRNA families associated with phase transition in Chinese jujube. *Acta Horticulturae Sinica*, 49: 23–40. (in Chinese)
- Liu, Y., Teng, C., Xia, R., Meyers, B.C., 2020. PhasiRNAs in Plants: Their Biogenesis, genic sources, and roles in stress responses, development, and reproduction. *Plant Cell*, 32: 3059–3080.
- Mallory, A., Vaucheret, H., 2010. Form, function, and regulation of ARGONAUTE proteins. *Plant Cell*, 22: 3879–3889.
- Mano, S., Nakamura, T., Kondo, M., Miwa, T., Nishikawa, S.I., Mimura, T., Nagatani, A., Nishimura, M., 2014. The plant organelles database 3 (PODB3) update 2014: Integrating electron micrographs and new options for plant organelle research. *Plant Cell Physiol*, 55: 1–9.
- Miura, K., Ikeda, M., Matsubara, A., Song, X.J., Ito, M., Asano, K., Matsuoka, M., Kitano, H., Ashikari, M., 2010. *OsSPL14* promotes panicle branching and higher grain productivity in rice. *Nat Genet*, 42: 545–549.
- Pokhrel, S., Huang, K., Bélanger, S., Zhan, J., Caplan, J.L., Kramer, E.M., Meyers, B.C., 2021. Pre-meiotic 21-nucleotide reproductive phasiRNAs emerged in seed plants and diversified in flowering plants. *Nat Commun*, 12: 4941.
- Seto, Y., Yasui, R., Kameoka, H., Tamiru, M., Cao, M., Terauchi, R., Sakurada, A., Hirano, R., Kisugi, T., Hanada, A., Umehara, M., Seo, E., Akiyama, K., Burke, J., Takeda-Kamiya, N., Li, W., Hirano, Y., Hakoshima, T., Mashiguchi, K., Noel, J.P., Kyoizuka, J., Yamaguchi, S., 2019. Strigolactone perception and deactivation by a hydrolase receptor DWARF14. *Nat Commun*, 10: 191.
- Shahid, S., Kim, G., Johnson, N.R., Wafula, E., Wang, F., Coruh, C., Bernal-Galeano, V., Phifer, T., Depamphilis, C.W., Westwood, J.H., Axtell, M.J., 2018. MicroRNAs from the parasitic plant *Cuscuta campestris* target host messenger RNAs. *Nature*, 553: 82–85.
- Sharma, A., Badola, P.K., Bhatia, C., Sharma, D., Trivedi, P.K., 2020. Primary transcript of miR858 encodes regulatory peptide and controls flavonoid biosynthesis and development in *Arabidopsis*. *Nat Plants*, 6: 1262–1274.
- Shuai, P., Su, Y., Liang, D., Zhang, Z., Xia, X., Yin, W., 2016. Identification of phasiRNAs and their drought- responsiveness in *Populus trichocarpa*. *FEBS Lett*, 590: 3616–3627.
- Song, X., Lu, Z., Yu, H., Shao, G., Xiong, J., Meng, X., Jing, Y., Liu, G., Xiong, G., Duan, J., Yao, X.F., Liu, C.M., Li, H., Wang, Y., Li, J., 2017. IPA1 functions as a downstream transcription factor repressed by D53 in strigolactone signaling in rice. *Cell Res*, 27: 1128–1141.
- Sun, Q., Liu, X., Yang, J., Liu, W., Du, Q., Wang, H., Fu, C., Li, W.X., 2018. MicroRNA528 affects lodging resistance of maize by regulating lignin biosynthesis under nitrogen-luxury conditions. *Mol Plant*, 11: 806–814.

- Sun, Q., Xie, Y., Li, H., Liu, J., Geng, R., Wang, P., Chu, Z., Chang, Y., Li, G., Zhang, X., 2021. Cotton *GhBRC1* regulates branching, flowering, and growth by integrating multiple hormone pathways. *Crop J*, 10: 75-87.
- Thimmappa, R., Geisler, K., Louveau, T., O'Maille, P., Osbourn, A., 2014. Triterpene biosynthesis in plants. *Annu Rev Plant Biol*, 65: 225–257.
- Wang, B., Tan, H.W., Fang, W., Meinhardt, L.W., Mischke, S., Matsumoto, T., Zhang, D., 2015. Developing single nucleotide polymorphism (SNP) markers from transcriptome sequences for identification of longan (*Dimocarpus longan*) germplasm. *Hortic Res*, 2: 1–10.
- Wang, J.W., Czech, B., Weigel, D., 2009. miR156-regulated *SPL* transcription factors define an endogenous flowering pathway in *Arabidopsis thaliana*. *Cell*, 138: 738–749.
- Wang, L., Wang, B., Yu, H., Guo, H., Lin, T., Kou, L., Wang, A., Shao, N., Ma, H., Xiong, G., Li, X., Yang, J., Chu, J., Li, J., 2020. Transcriptional regulation of strigolactone signalling in *Arabidopsis*. *Nature*, 583: 277–281.
- Wu, G., Park, M.Y., Conway, S.R., Wang, J.W., Weigel, D., Poethig, R.S., 2009. The sequential action of miR156 and miR172 regulates developmental timing in *Arabidopsis*. *Cell*, 138: 750–759.
- Xia, R., Chen, C., Pokhrel, S., Ma, W., Huang, K., Patel, P., Wang, F., Xu, J., Liu, Z., Li, J., Meyers, B.C., 2019. 24-nt reproductive phasiRNAs are broadly present in angiosperms. *Nat Commun*, 10: 1–8.
- Xia, R., Meyers, B.C., Liu, Zhongchi, Beers, E.P., Ye, S., Liu, Zongrang, 2013. MicroRNA superfamilies descended from miR390 and their roles in secondary small interfering RNA biogenesis in eudicots. *Plant Cell*, 25: 1555–1572.
- Xia, R., Xu, J., Meyers, B.C., 2017. The emergence, evolution, and diversification of the miR390-*TAS3-ARF* pathway in land plants. *Plant Cell*, 29: 1232–1247.
- Xia, R., Ye, S., Liu, Z.R., Meyers, B.C., Liu, Z.C., 2015. Novel and recently evolved microRNA clusters regulate expansive *F-BOX* gene networks through phased small interfering RNAs in wild diploid strawberry. *Plant Physiol*, 169: 594–610.
- Xie, Y., Liu, Y., Ma, M., Zhou, Q., Zhao, Y., Zhao, B., Wang, B., Wei, H., Wang, H., 2020. *Arabidopsis* *FHY3* and *FAR1* integrate light and strigolactone signaling to regulate branching. *Nat Commun*, 11: 1–13.
- Yang, R., Li, P., Mei, H., Wang, D., Sun, J., Yang, C., Hao, L., Cao, S., Chu, C., Hu, S., Song, X., Cao, X., 2019. Fine-tuning of MiR528 accumulation modulates flowering time in rice. *Mol Plant*, 12: 1103–1113.
- Yao, R., Ming, Z., Yan, L., Li, S., Wang, F., Ma, S., Yu, C., Yang, M., Chen, Li, Chen, Linhai, Li, Y., Yan, C., Miao, D., Sun, Z., Yan, J., Sun, Y., Wang, L., Chu, J., Fan, S., He, W., Deng, H., Nan, F., Li, J., Rao, Z., Lou, Z., Xie, D., 2016. DWARF14 is a non-canonical hormone receptor for strigolactone. *Nature*, 536: 469–473.
- Yao, S., Yang, Z., Yang, R., Huang, Y., Guo, G., Kong, X., Lan, Y., Zhou, T., Wang, H., Wang, W., Cao, X., Wu, J., Li, Y., 2019. Transcriptional regulation of miR528 by OsSPL9 orchestrates antiviral response in rice. *Mol Plant*, 12: 1114–1122.
- Zhai, J., Jeong, D.H., de Paoli, E., Park, S., Rosen, B.D., Li, Y., González, A.J., Yan, Z., Kitto, S.L., Grusak, M.A., Jackson, S.A., Stacey, G., Cook, D.R., Green, P.J., Sherrier, D.J., Meyers, B.C., 2011. MicroRNAs as master regulators of the plant *NB-LRR* defense gene family via the production of phased, *trans*-acting siRNAs. *Genes Dev*, 25: 2540–2553.
- Zhang, L.B., Xia H., Wu J.S., Li M.T., 2022a. MiRNA identification, characterization and integrated network analysis for flavonoid biosynthesis in Brassicacoraphanus. *Hortic Plant J*, 8: 319–327.
- Zhang, Q., Ma, C., Zhang, Y., Gu, Z., Li, W., Duan, X., Wang, Shengnan, Hao, L., Wang, Y., Wang, Shengyuan, Li, T., 2018. A single-nucleotide polymorphism in the promoter of a hairpin rna contributes to alternaria alternata leaf spot resistance in apple (*Malus × domestica*). *Plant Cell*, 30: 1924–1942.
- Zhang, Q.W., Yang, X., Li, F., Deng, Y.T., 2022b. Advances in miRNA-mediated growth and development regulation in horticultural crops. *Acta Horticulturae Sinica*, 49: 1145–1161. (in Chinese)
- Zhang, Y., Waseem, M., Zeng, Z., Xu, J., Chen, C., Liu, Y., Zhai, J., Xia, R., 2021. MicroRNA482/2118, a miRNA superfamily essential for both disease resistance and plant development. *New Phytol*, 233: 2047-2057.
- Zhu, H., Chen, C., Zeng, J., Yun, Z., Liu, Y., Qu, H., Jiang, Y., Duan, X., Xia, R., 2020. MicroRNA528, a hub regulator modulating ROS homeostasis via targeting of a diverse set of genes encoding copper-containing proteins in monocots. *New Phytol*, 225: 385–399.